Artificial phonon-plasmon polariton at the interface of piezoelectric metamaterials and semiconductors

Xuejin Zhang, Dongmin Wu, Cheng Sun, and Xiang Zhang*
NSF Nanoscale Science and Engineering Center (NSEC), 3112 Etcheverry Hall, University of California, Berkeley, California 94720, USA

(Received 6 June 2007; published 13 August 2007)

We studied a polariton formed at the interface between a piezoelectric metamaterial and a semiconductor or metallic metamaterial. The piezoelectric metamaterial consists of periodically poled domains that has an optical phonon frequency in the terahertz ranges. When the piezoelectric metamaterial is in contact with a semiconductor or metallic metamaterial substrate, the coupling between the metamaterial's optical phonons and the substrate's plasmons results in the formation of a type of artificial surface polariton: phonon-plasmon polariton. The effective dielectric constant of the piezoelectric metamaterial is theoretically derived and the strong dispersion and band gap phenomena of the phonon-plasmon polariton are investigated. The artificial surface phonon-plasmon polariton may offer opportunities in optical science such as acoustic excitation of surface plasmons and vice versa.

DOI: 10.1103/PhysRevB.76.085318 PACS number(s): 73.20.Mf, 63.20.Ls, 71.36.+c, 77.65.−j

A polariton is a coupled mode of the electromagnetic (EM) field and the internal degrees of freedom of the medium.[1] The EM energy can be strongly confined and form interface guided modes known as surface polaritons. The surface phonon polaritons have shown some interesting physics such as coherent light emission from thermal sources.[2] Surface plasmon polaritons (SPPs), on the other hand, have generated significant interest recently related to surface enhanced Raman scattering,[3] extraordinary transmission of light through subwavelength holes in metal films,[4] and superlens effect via excitation of surface resonances.[5]

Plasmonic effects have been investigated,[6] including propagation of SPPs on corrugated metal wires,[7] in band gap structures,[8] and in random nanostructures.[9] The methods of changing the dielectric constant of one interfacial medium were also developed for controlling the propagation of SPPs.[10] Similar to the cases in photonics,[11] the polaritonic effects should be further considered under strongly dispersive conditions. The band gaps and significantly reduced group velocities of surface polaritons can be realized by the phonon-phonon coupling, plasmon-plasmon coupling, and phonon-plasmon coupling.[12] The frequency at which the coupling occurs solely depends on the material properties available in the nature. In most cases, the coupling is limited to high frequency ranged from infrared to ultraviolet spectrum. Especially for surface phonon-plasmon coupling, due to the large frequency mismatch between optical phonons and free electron plasmons, only very limited cases have been studied.[12] Recently discovered metamaterials provide a new route to design optical properties that do not exist in the nature.[13–16] Therefore, it is possible now to explore the phenomena of surface phonon-plasmon resonant coupling in terahertz (THz) or microwave frequencies.

This paper reports a surface polariton formed from the interaction between a piezoelectric metamaterial, which supports optical phonons at lower frequency than that of a natural material, and a doped semiconductor or metallic metamaterial, which has surface plasmons at the same frequency range. It is known that the zone-folding effect can introduce low frequency optical phonons with the aid of artificial periodic structures.[17] Furthermore, in piezoelectric periodic structures, the vibrations can excite additional polarization due to the piezoelectric effect.[18] Thus, the piezoelectric periodic structures can provide polar artificial optical phonons at desired frequencies, which could resonantly couple with surface EM field. This strong coupling results in a new hybrid polariton that involves artificial lattice vibration from the metamaterial and collective charge oscillation in the semiconductor or metallic metamaterial at the interface, namely, surface phonon-plasmon polariton. The frequency position of these optical phonons depends on the periodicity of the piezoelectric components and thus is tunable by changing the geometry parameters.

We choose a simple layered structure to demonstrate such a coupling effect and the resulting polariton phenomenon. A piezoelectric metamaterial film (medium 2) formed by a one-dimensional (1D) periodic structure lies upon a semi-infinite semiconductor or metallic metamaterial substrate (medium 3), as shown in Fig. 1 [elsewhere is vacuum (medium 1)]. The piezoelectric metamaterial is composed of two alternating components arranged along the x axis. The widths of the

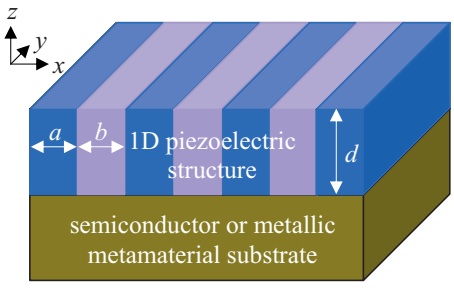

FIG. 1. (Color online) Schematic of a 1D piezoelectric metamaterial film in contact with a semi-infinite semiconductor or metallic metamaterial substrate. The stripes periodically arranged along the x axis represent two components with different piezoelectric coefficients. a and b denote the widths of two components and d the thickness of the film.

two components are a and b, while the thickness of the film is d, and the period of the piezoelectric metamaterial is $\Lambda = a+b$. As shown below, the piezoelectric metamaterial can interact with the EM field as long as the piezoelectric coefficient is modulated along the x direction. In our design, the two components are modulated such that their piezoelectric coefficients have equal absolute values but opposite signs, and there are no other modulated parameters to create conventional photonic or phononic band gaps. Such a configuration is feasible in experiments, e.g., it can be fabricated with poled ferroelectric domains by an external electric field.[19]

More specifically, we assume that the two components of the piezoelectric metamaterial are nonmagnetic crystals with symmetry of 6*mm* point groups whose c axes are normal to the substrate, and the piezoelectric coefficients change signs from one component to the next. We consider a p-polarized incident EM plane waves (electric vector $\boldsymbol{E}$ in the xz plane) with angular frequency ω and parallel wave vector k_x. Due to the piezoelectric effect, vibration waves can be excited in the piezoelectric metamaterial film by the incident EM plane waves. In this case, additional electric polarization induced by the piezoelectric effect will contribute to the effective dielectric function of the metamaterial film. According to the acoustic motion equations and piezoelectric equations,[20] the change of the dielectric function in response to the piezoelectric effect can be estimated. If $|k_{z2}|d \ll 1$, the fields vary approximately only with the x coordinate within the piezoelectric metamaterial film. The related equations thus can be simplified as

$$P_1(x,t) = e_{15}(x)S_5(x,t) + \varepsilon_0(\varepsilon_{11}^S - 1)E_1(x,t),$$

$$P_3(x,t) = e_{31}(x)S_1(x,t) + \varepsilon_0(\varepsilon_{33}^S - 1)E_3(x,t),$$

$$T_1(x,t) = C_{11}^E S_1(x,t) - e_{31}(x)E_3(x,t),$$

$$T_5(x,t) = C_{44}^E S_5(x,t) - e_{15}(x)E_1(x,t),$$

$$\rho\frac{\partial^2 S_1(x,t)}{\partial t^2} = \frac{\partial^2 T_1(x,t)}{\partial x^2},$$

$$\rho\frac{\partial^2 S_5(x,t)}{\partial t^2} = \frac{\partial^2 T_5(x,t)}{\partial x^2}, \tag{1}$$

where $P_{1,3}$, $S_{1,5}$, $E_{1,3}$, and $T_{1,5}$ are the field components of electric polarization, strain, electric field, and stress, respectively. $e_{ij}(x), \varepsilon_0, \varepsilon_{ij}^S, C_{ij}^E$, and ρ are the piezoelectric coefficient, vacuum permittivity, dielectric coefficient, elastic coefficient, and mass density, respectively. The high-order piezoelectric effect and the material damping are ignored in Eq. (1). $e_{ij}(x) = e_{ij}f(x) = e_{ij}\Sigma_m f_m \exp(iG_m x)$, with the reciprocal vector $G_m = 2\pi m/\Lambda$ (m is an integer) and the Fourier coefficient of the 1D piezoelectric metamaterial structure f_m ($f_0 = (a-b)/\Lambda$ and $f_m = 2\sin(m\pi a/\Lambda)/(m\pi)$ for $m \neq 0$). In Eq. (1), the additional electric polarization $e_{15}(x)S_5$ stands for the transverse metamaterial vibration case, and $e_{31}(x)S_1$ stands for the longitudinal metamaterial vibration case. For the polariton case, $k_x\Lambda \ll 1$, i.e., the polarization induced by metamaterial vibrations contributes to the dielectric function in the sense of a spatially averaged value. In this argument, we have $D_1 = \varepsilon_{11}(k_x,\omega)E_1$ and $D_3 = \varepsilon_{33}(k_x,\omega)E_3$, where the effective dielectric functions $\varepsilon_{11}(k_x,\omega)$ and $\varepsilon_{33}(k_x,\omega)$ of the piezoelectric metamaterial have the following analytical form:

$$\varepsilon_{11}(k_x,\omega) = \varepsilon_{11}^S + \frac{e_{15}^2}{\varepsilon_0}\sum_{m=0,\pm1,\pm2,\ldots}\frac{(k_x+G_m)^2}{C_{44}^E(k_x+G_m)^2 - \rho\omega^2}f_m^2,$$

$$\varepsilon_{33}(k_x,\omega) = \varepsilon_{33}^S + \frac{e_{31}^2}{\varepsilon_0}\sum_{n=0,\pm1,\pm2,\ldots}\frac{(k_x+G_n)^2}{C_{11}^E(k_x+G_n)^2 - \rho\omega^2}f_n^2. \tag{2}$$

In Eq. (2), the second term on the right of the first equation arises from the transverse metamaterial vibrations, while that of the second equation from longitudinal metamaterial vibrations. E_1 couples to the electric polarization associated with transverse metamaterial vibrations, while E_3 couples to the electric polarization associated with longitudinal metamaterial vibrations.

The dispersion relation of surface polaritons for the system in Fig. 1 can be derived from the electromagnetic boundary conditions or the resonant condition indicated by the expression of the reflectivity in terms of Fresnel's equations. That is, the dispersion curves can be outlined in view of the value of the reflectivity. In the wake of Pendry's proof that evanescent waves can be amplified,[21] the transmissivity is also quite applicable to lay out the dispersion curves and sets the direction for the design of polaritonic or plasmonic devices, such as superlenses. Here, we calculate the transmissivity with respect to different wave vectors and angular frequencies to map the dispersion of surface polaritons.

For comparison, we consider two cases for the film: with and without modulations of piezoelectric coefficients. We take a well-studied material $LiNbO_3$ as an example. The crystal is textured with the c axis normal to the substrate. Its crystallographic symmetry is equivalent to a 6*mm* point group. In spite of the difference between the bulk and film as well as between the single crystal and ceramic, experiments show close values of their material parameters. We use the values of elastic, piezoelectric, and dielectric coefficients the same as those of a single domain $LiNbO_3$ crystal in our calculation.[20] Figure 2(a) shows the dispersion curve of the SPP accompanied by the transmissivity for a similar system shown in Fig. 1, where a 200-nm-thick $LiNbO_3$ film, textured with the c axis normal to the substrate, replaces the piezoelectric metamaterial film. The dielectric function of the substrate is calculated using the simple Drude model: $\varepsilon_3 = 1 - \omega_p^2/\omega^2$, where ω_p is the plasma frequency. In this paper, the plasma frequency $f_p = \omega_p/(2\pi)$ of the semiconductor substrate is assumed as 1.5 THz, which corresponds to a moderate doping level of about 10^{16} cm^{-3} in n-type silicon.[22] The parallel wave vector k_x is also normalized by $k_p = \omega_p/c$ in Fig. 2(a). Interestingly, zero and negative group velocities at larger parallel wave vectors k_x are possible in the thin film structure, as shown in a previous study.[23] The dispersion curve is situated between that of surface polaritons at a

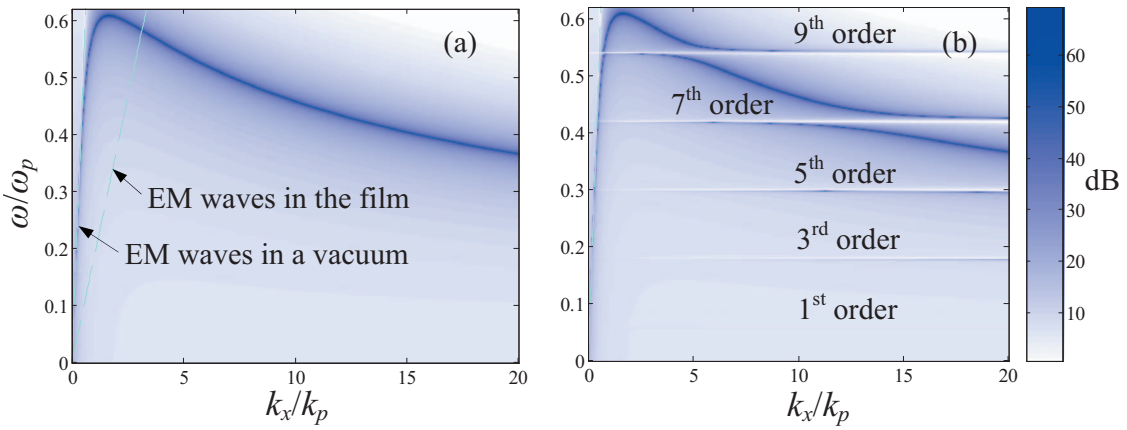

FIG. 2. (Color online) The dispersion curves of (a) surface plasmon polaritons for a similar layered system shown in Fig. 1, where the metamaterial film is replaced by a 200-nm-thick $LiNbO_3$ film textured with the c axis normal to the substrate, and (b) surface phonon-plasmon polaritons for the layered system shown in Fig. 1. Two components in Fig. 1 correspond to a textured 200-nm-thick $LiNbO_3$ of width of 20 nm with the $+c$ axis along the $+z$ direction and the $-c$ axis along the $+z$ direction. The labels denote the order numbers of transverse "phonon polaritons" woven into the surface plasmon polaritons.

vacuum-substrate interface and that of surface polaritons at a textured $LiNbO_3$-substrate interface, with relative position being determined by the film thickness. For small parallel wave vector k_x (low frequency), the electric field of surface polaritons extends a large (compared to the film thickness) distance into the vacuum, and the dispersion curve is dominated by that of surface polaritons for the semi-infinite vacuum on the substrate. When the parallel wave vector k_x increases, the penetration depth of the field into the film and vacuum regions decreases. Hence, the dispersion curve shifts to that of surface polaritons for semi-infinite textured $LiNbO_3$ on substrate, which has a lower SPP resonant frequency than the case of vacuum. The effect of periodic modulation in the thin piezoelectric film introduces additional band gap structures on the original dispersion curve of the unmodulated system.

According to Eq. (2), the "phonon polaritons" associated with SPP waves will occur around $\omega^2 = G_m^2 v^2$, where $v = (C_{44}^E/\rho)^{1/2}$ or $(C_{11}^E/\rho)^{1/2}$ is the phase velocity of the transverse or longitudinal metamaterial vibration wave. The fundamental resonant frequencies are $f_T = (C_{44}^E/\rho)^{1/2}/\Lambda$ and $f_L = (C_{11}^E/\rho)^{1/2}/\Lambda$. In addition, the resonant states are distributed equidistantly along the frequency axis, in accordance with the period of the metamaterial structure. We assume that the 200-nm-thick metamaterial film consists of two alternately textured $LiNbO_3$ stripes, with the $+c$ axis and $-c$ axis along the $+z$ direction. Each stripe has a width of 20 nm, i.e., the period $\Lambda = a + b = 40$ nm (which is feasible according to Ref. 19). The dispersion relation is calculated and illustrated in Fig. 2(b). Although the outline of the dispersion curve in Fig. 2(a) still exists, it has undergone a dramatic transformation after introducing the piezoelectric metamaterial, as a result of the resonant coupling between the SPPs and polar artificial phonons. The obvious phonon polaritons in Fig. 2(b) originate from the transverse metamaterial vibrations. The longitudinal metamaterial vibrations cannot be discerned on the scale of Fig. 2(b) because of the very weak electromechanical coupling coefficient, 7.67×10^{-4} for such vibrations (0.586 for the transverse case). In our case, when $a = b$, only the odd-order Fourier coefficient f_m in Eq. (2) has a nonzero value, which explains the order of resonance indicated in Fig. 2(b). There are three curves but one band gap

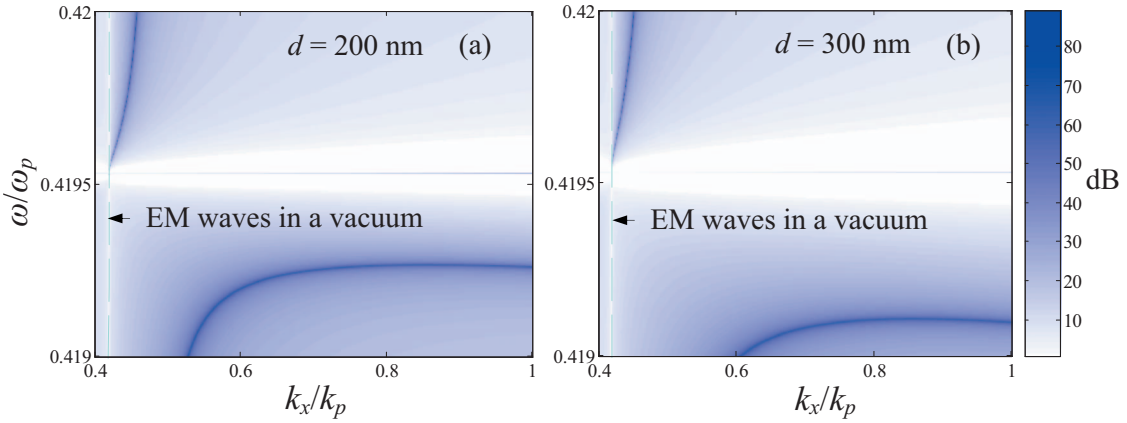

FIG. 3. (Color online) The close-up dispersion curves of the seventh-order surface phonon-plasmon polariton in Fig. 2(b). The thicknesses of the piezoelectric metamaterial film are (a) 200 nm and (b) 300 nm.

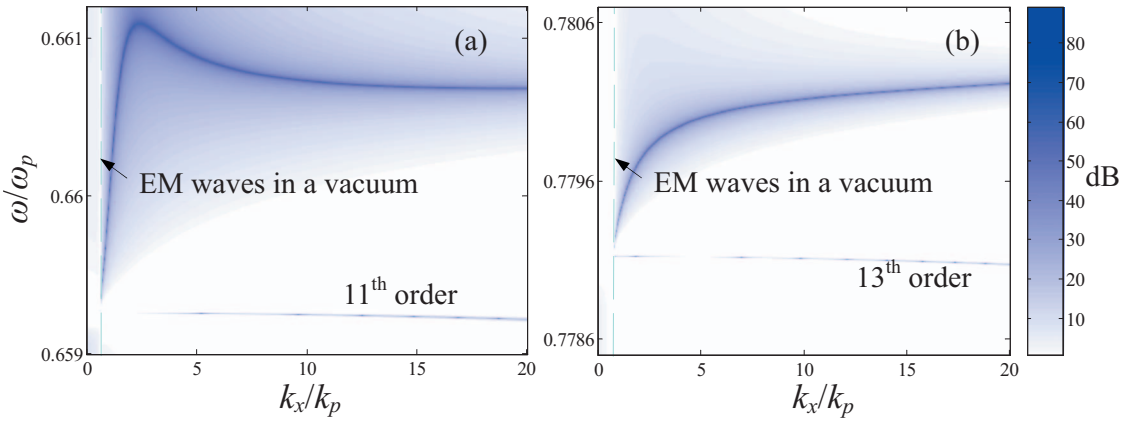

FIG. 4. (Color online) The dispersion curves of (a) the 11th-order and (b) the 13th-order surface polaritons. The system is the same as that of Fig. 2(b).

for surface modes of the phonon-plasmon coupling. This characteristic is revealed in Fig. 3. In contrast to the bulk one, the upper band gap vanishes and the lower band gap is widened. This lower band gap changes with the order number m of phonon polaritons and the thickness of the piezoelectric metamaterial film [see Figs. 3(a) and 3(b)]. The SPPs and the optical phonons are simultaneously forbidden to propagate in the band gap, i.e., no surface wave mode exists and the incident wave will be totally reflected. It is worth noticing that the surface states are not restricted in the regime of SPPs shown in Fig. 2(a). They take place near any resonant frequencies of the piezoelectric metamaterial. However, at those frequencies that are higher than the SPP resonant frequency for vacuum-substrate interface, the coupling between the artificial optical phonon and the EM field results in surface phonon polaritons. Figure 4 gives dispersion relations of surface polaritons at higher orders. The frequency range of Fig. 4(a) [4(b)] lies within (out of) that of SPPs for the interface of the semi-infinite vacuum and substrate. This difference makes the negative group velocity appear in Fig. 4(a) but disappears in Fig. 4(b) for the upper branch.

When losses are taken into account, the transmission becomes weaker and the band gap can be less pronounced. Generally, the losses increase with parallel momentum along the surface because the phonon-plasmon polariton concentrates more inside the substrate at higher k_x. The size of band gaps is determined by material constants of the piezoelectric metamaterial (piezoelectric, elastic, and dielectric coefficients) and the order number m of phonon polaritons, and broader band gaps can be realized by choosing piezoelectric metamaterials with larger electromechanical coupling coefficients. Experimentally, a newly developed THz time-domain spectroscopy is an effective approach of measuring the propagation of such surface polaritons.[24] Furthermore, the THz Fourier transform infrared (FTIR) spectroscopy or the transmission phase time approach[25] may have the possibility to conduct such experiments. For instance, the typical frequency resolution of a high resolution THz FTIR is 0.020 cm^{-1} (Sciencetech model SPS-300), which is about 1 order less than the band gap shown in Fig. 3. Therefore, this band gap is measurable.

It should be noted that the size of building components of the piezoelectric metamaterial is much smaller than the wavelength of the surface polaritons, which makes it very different from the band gap structure based on the Bragg reflection. Instead, the band gaps in the dispersion curve are due to resonant coupling between the polar artificial phonons and SPPs. Owing to this strong coupling, the artificial surface phonon-plasmon polaritons can be excited by acoustic waves. Especially, it is possible to electrically excite the artificial phonons at piezoelectric metamaterials, which provides another way to control and manipulate plasmonic characteristics such as excitation and propagation.

In summary, the dispersion and band gap characteristics of THz artificial surface phonon-plasmon polariton were investigated. We studied the coupling between surface plasmons of semiconductors or metallic metamaterials and optical phonons of piezoelectric metamaterials at the interface. Both the metamaterial structure and the piezoelectric components are found essential for the coupling and resulting polaritonic properties. Due to the scalability of the optical response of the piezoelectric metamaterials, it is relatively easy to extend this artificial surface polaritons into the microwave range.

This work was supported by AFOSR MURI program (Grant No. FA9550-04-1-0434) and NSF Nanoscale Science and Engineering Center (NSEC) (Grant No. DMI-0327077).

*xiang@berkeley.edu

[1] D. L. Mills and E. Burstein, Rep. Prog. Phys. **37**, 817 (1974).
[2] J.-J. Greffet, R. Carminati, K. Joulain, J.-P. Mulet, S. Mainguy, and Y. Chen, Nature (London) **416**, 61 (2002).
[3] M. Fleischmann, P. J. Hendra, and A. J. McQuillan, Chem. Phys. Lett. **26**, 163 (1974); F. J. García-Vidal and J. B. Pendry, Phys. Rev. Lett. **77**, 1163 (1996).
[4] T. W. Ebbesen, L. J. Lezec, H. F. Chaemi, T. Thio, and P. A. Wolff, Nature (London) **391**, 667 (1998); L. Martín-Moreno, F. J. García-Vidal, H. J. Lezec, K. M. Pellerin, T. Thio, J. B. Pendry, and T. W. Ebbesen, Phys. Rev. Lett. **86**, 1114 (2001).
[5] N. Fang, H. Lee, C. Sun, and X. Zhang, Science **308**, 534 (2005).
[6] H. Ditlbacher, J. R. Krenn, G. Schider, A. Leitner, and F. R. Aussenegg, Appl. Phys. Lett. **81**, 1762 (2002); J. M. Pitarke, V. M. Silkin, E. V. Chulkov, and P. M. Echenique, Rep. Prog. Phys. **70**, 1 (2007).
[7] S. A. Maier, S. R. Andrews, L. Martín-Moreno, and F. J. García-Vidal, Phys. Rev. Lett. **97**, 176805 (2006).
[8] S. I. Bozhevolnyi, J. Erland, K. Leosson, P. M. W. Skovgaard, and J. M. Hvam, Phys. Rev. Lett. **86**, 3008 (2001).
[9] S. I. Bozhevolnyi, V. S. Volkov, and K. Leosson, Phys. Rev. Lett. **89**, 186801 (2002).
[10] A. V. Krasavin and N. I. Zheludev, Appl. Phys. Lett. **84**, 1416 (2004); Y. Wang, S. D. Russell, and R. L. Shimabukuro, J. Appl. Phys. **97**, 023708 (2005).
[11] K. C. Huang, P. Bienstman, J. D. Joannopoulos, K. A. Nelson, and S. Fan, Phys. Rev. Lett. **90**, 196402 (2003); , Phys. Rev. B **68**, 075209 (2003).
[12] *Electromagnetic Surface Modes*, edited by A. D. Boardman (Wiley, Chichester, 1982).
[13] R. A. Shelby, D. R. Smith, and S. Schultz, Science **292**, 79 (2001).
[14] J. B. Pendry, A. J. Holden, W. J. Stewart, and I. Youngs, Phys. Rev. Lett. **76**, 4773 (1996).
[15] T. J. Yen, W. J. Padilla, N. Fang, D. C. Vier, D. R. Smith, J. B. Pendry, D. N. Basov, and X. Zhang, Science **303**, 1494 (2004).
[16] N. Fang, D. J. Xi, J. Y. Xu, M. Ambati, W. Srituravanich, C. Sun, and X. Zhang, Nat. Mater. **5**, 452 (2006).
[17] G. P. Srivastava, *The Physics of Phonons* (Adam Hilger, New York, 1990).
[18] Y. Y. Zhu, X. J. Zhang, Y. Q. Lu, Y. F. Chen, S. N. Zhu, and N. B. Ming, Phys. Rev. Lett. **90**, 053903 (2003); X. J. Zhang, R. Q. Zhu, J. Zhao, Y. F. Chen, and Y. Y. Zhu, Phys. Rev. B **69**, 085118 (2004).
[19] G. Rosenman, P. Urenski, A. Agronin, Y. Rosenwaks, and M. Molotskii, Appl. Phys. Lett. **82**, 103 (2003).
[20] B. A. Auld, *Acoustic Fields and Waves in Solids* (Wiley, New York, 1973).
[21] J. B. Pendry, Phys. Rev. Lett. **85**, 3966 (2000).
[22] M. van Exter and D. Grischkowsky, Phys. Rev. B **41**, 12140 (1990).
[23] M. I. Stockman, Nano Lett. **6**, 2604 (2006).
[24] J. Saxler, J. Gómez Rivas, C. Janke, H. P. M. Pellemans, P. Haring Bolivar, and H. Kurz, Phys. Rev. B **69**, 155427 (2004); J. Gómez Rivas, M. Kuttge, P. Haring Bolivar, H. Kurz, and J. A. Sánchez-Gil, Phys. Rev. Lett. **93**, 256804 (2004).
[25] E. H. El Boudouti, N. Fettouhi, A. Akjouj, B. Djafari-Rouhani, A. Mir, J. O. Vasseur, L. Dobrzynski, and J. Zemmouri, J. Appl. Phys. **95**, 1102 (2004).